ACCSCIENCE PUBLISHING

International Journal of Bioprinting

RESEARCH ARTICLE

Exosome immobilization of 3D-printed polycaprolactone scaffolds for bone tissue engineering

Ilwoo Jun[1], Ji-Young Ahn[2], Gna Ahn[2,3], Hye-Jung Kim[4], Junhyoung Ahn[1], Hyungjun Lim[1], Jae Jong Lee[1], and Su A Park[1]*

[1]Nano-Convergence Manufacturing Research Division, Korea Institute of Machinery and Materials (KIMM), Daejeon, Republic of Korea

[2]Department of Microbiology, College of Natural Science, Chungbuk National University, Cheongju, Republic of Korea

[3]School of Advanced Biosciences, Glocal Advanced Institute of Science and Technology, Changwon National University, Changwon, Republic of Korea

[4]Convergence Materials Research and Development Division, Korea Institute of Ceramic Engineering and Technology, Cheongju, Republic of Korea

Abstract

Biodegradable polymers are widely used in bone tissue engineering to repair bone defects by providing biocompatible scaffolds with good mechanical support. Among them, three-dimensional (3D)-printed polycaprolactone (PCL) is commonly used due to its biocompatibility and compressive stability. However, its hydrophobicity and lack of osteogenic cues limit cell attachment and osteogenic differentiation. To address these limitations, 3D-printed PCL scaffolds were coated with polydopamine (PDA) to increase hydrophilicity, and milk-derived exosomes (EXOs) were immobilized on the surface to promote cell proliferation and induce osteogenic differentiation, thereby producing PDA–EXO scaffolds. EXOs represent a cell-free alternative for delivering growth factors and microRNA cargo that provide osteogenic cues for bone regeneration. PDA–EXO scaffolds demonstrated greater cell viability and proliferation compared to PCL and PDA scaffolds due to the synergistic effects of the PDA coating and the EXOs. The PDA–EXO scaffolds also led to better osteogenic differentiation compared to the other scaffolds. Taken together, these findings indicate that PDA enhanced surface hydrophilicity and that milk-derived EXOs provided osteoinductive signals, thereby synergistically increasing cell proliferation and osteogenic differentiation while maintaining the scaffold's mechanical properties. PDA–EXO functionalization, therefore, represents a practical, cell-free strategy to enhance PCL scaffolds for bone tissue engineering.

Keywords: Polycaprolactone; 3D-printed; Polydopamine; Milk-derived exosome; Bone tissue engineering

***Corresponding author:**
Su A Park
(psa@kimm.re.kr)

Citation: Jun I, Ahn JY, Ahn G, *et al*. Exosome immobilization of 3D-printed PCL scaffolds for bone tissue engineering. *Int J Bioprint*. 2026:12(2):026030021. doi: 10.36922/IJB026030021

Received: January 13, 2026

Revised: February 1, 2026

Accepted: February 6, 2026

Published online: April 6, 2026

1. Introduction

Exosomes (EXOs) are nanoscale membranous vesicles with therapeutic potential in tissue engineering and regenerative medicine.[1] They contain the proteins, lipids, mRNA, and microRNAs (miRNAs) involved in intercellular signaling.[2] Through intercellular communication, EXOs transfer bioactive molecules and activate target cells.[1,2] Milk-derived EXOs have been reported to exhibit low immunogenicity and high biocompatibility.[3] Furthermore, several studies have shown that EXOs enhance osteoblast proliferation and promote osteogenic differentiation *in vitro*, as indicated by increased expression of canonical osteogenic markers, elevated alkaline phosphatase (ALP) activity, and calcium deposition.[2,4,5] These findings imply that EXOs contribute to bone regeneration.

Scaffolds for bone regeneration are designed to have high porosity and an interconnected structure to support cell infiltration, facilitate transfer of oxygen and nutrients, and mimic the architecture of native bone.[6,7] In addition, the materials used for three-dimensional (3D)-printed bone scaffolds must ensure both structural integrity and biocompatibility.[8] Polycaprolactone (PCL) is a biocompatible, biodegradable synthetic polymer with mechanical properties that are suitable for structural support.[9] However, PCL scaffolds exhibit limited bioactivity, particularly in promoting cell adhesion and osteogenic differentiation. Recent studies have therefore explored combining PCL scaffolds with EXOs to enhance bone regeneration.[9-11] EXOs deliver proteins and regulatory RNAs that support cell adhesion, proliferation, and osteogenic differentiation.[12] EXO-functionalized scaffolds have been shown to promote these cellular activities and modulate immune responses toward a regenerative phenotype, thereby significantly improving bone regeneration.[11,13] Therefore, combining PCL scaffolds with milk-derived EXOs enhances scaffold bioactivity, including improved cell attachment and osteoinductive potential.

Polycaprolactone is widely used to fabricate 3D-printed scaffolds for bone tissue engineering and regeneration.[14] However, PCL is inherently hydrophobic due to the absence of polar functional groups.[10] As a result, its surface exhibits low hydrophilicity, limiting cell adhesion and reducing osteogenic potential.[15] To overcome this limitation, polydopamine (PDA) coating is commonly used to enhance surface hydrophilicity and bioactivity.[16] PDA surface modification improves scaffold hydrophilicity and promotes cell adhesion and proliferation on PCL scaffolds.[17-19] Moreover, PDA provides abundant catechol and amine groups that facilitate stable interactions with bioactive molecules, enabling effective immobilization of EXOs on PDA-coated surfaces via non-covalent interactions.[20] This immobilization helps to retain EXOs on the scaffold, enhancing their stability and prolonging their bioactivity, to support osteogenic differentiation and bone regeneration.[21] Accordingly, PDA represents a promising strategy for maintaining localized and sustained EXO bioactivity on bone scaffolds.[21,22]

In our study, milk-derived EXOs, which support bone regeneration, were immobilized on the surface of biodegradable PDA-coated scaffolds to fabricate functionalized bone scaffolds. We investigated the osteogenic effects of these PDA–EXO composite scaffolds for bone regeneration. First, scaffolds designed to mimic native bone architecture were fabricated using 3D printing technology with PCL. The printed PCL scaffolds were then coated with PDA to enhance surface hydrophilicity and promote cell attachment. Finally, EXOs were immobilized onto the PDA-coated scaffolds to create PDA–EXO scaffolds. The resulting composite scaffolds were evaluated for cell viability, proliferation, and osteogenic differentiation (Figure 1).

2. Materials and methods

2.1. Materials

Polycaprolactone (molecular weight: 37,000; Polysciences, USA) and dopamine hydrochloride (Sigma-Aldrich, USA) were used to fabricate scaffolds. Dulbecco's Modified Eagle's Medium (DMEM; Gibco Life Technologies, USA), fetal bovine serum (FBS; Gibco Life Technologies, USA), 1% penicillin, and alpha minimal essential medium (α-MEM; Gibco Life Technologies, USA) were used for cell culture. Acetic acid (AA; Merck, USA) and Dulbecco's phosphate-buffered saline (PBS; Welgene, Republic of Korea) were used for EXO isolation.

2.2. Isolation of milk-derived exosomes

Low-temperature pasteurized low-fat milk (Pasteur milk, Lottefood, Republisc of Korea) was purchased from a local market. Milk-derived EXOs were isolated using a modification of the protocol described previously.[23] Briefly, milk was centrifuged at 3,000 × *g* for 30 min at 4 °C to remove the upper fat layer. Then, 1% (v/v) AA was added, and the mixture was incubated at room temperature for 5 min. The samples were subsequently centrifuged at 10,000 × *g* for 10 min at 4 °C, and the resulting whey was filtered through a 0.22-μm bottle-top vacuum filter (Corning, USA). The filtered whey was ultracentrifuged at 200,000 × g for 60 min at 4 °C (Beckman Coulter, USA) and washed in Dulbecco's PBS under the same conditions. The isolated milk-derived EXOs were aliquoted and stored at −80 °C until use.

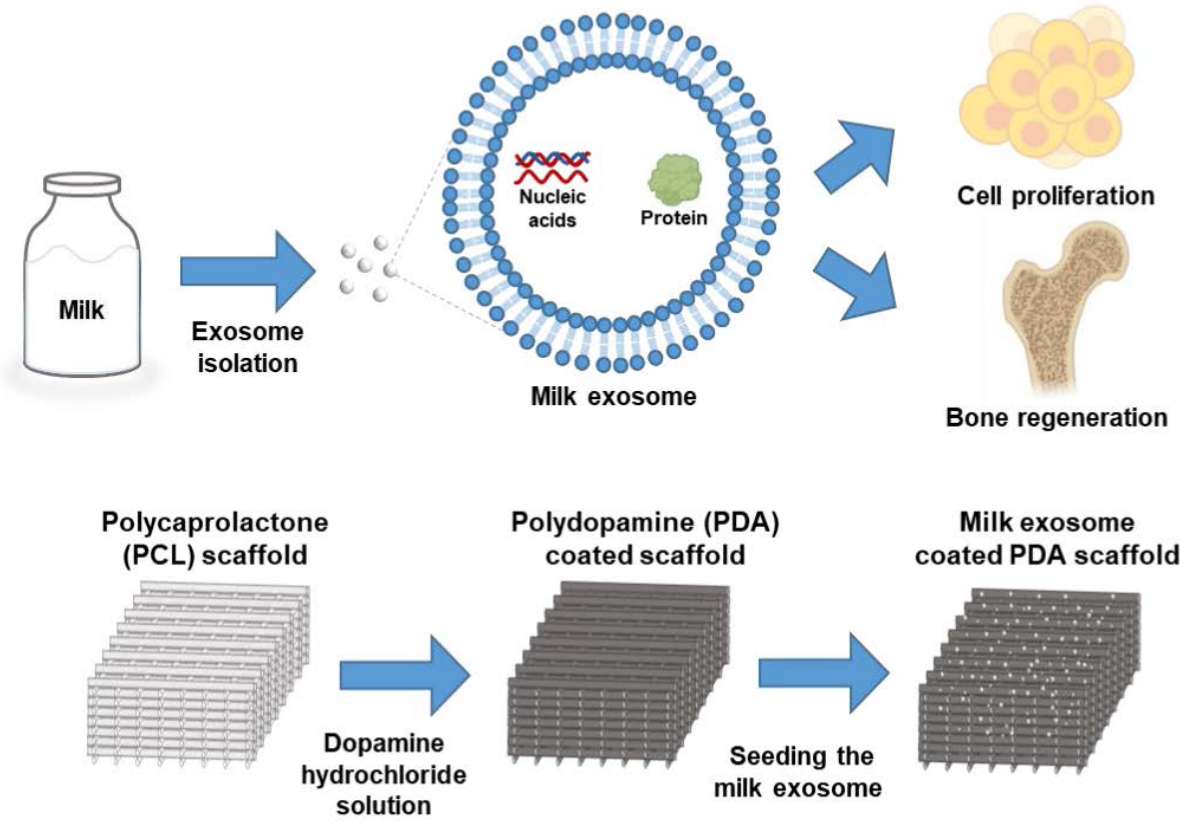

Figure 1. Schematic illustration of the various functions of milk-derived exosomes (EXOs) and the procedure for preparing milk-derived EXO-coated polydopamine scaffold

The size and concentration of EXOs were measured using a tunable resistive pulse-sensing measurement system (qNano Gold, Izon Science, New Zealand). Cryo-electron microscopy (cryo-EM; Tecnai G2 F20 TWIN TMP, FEI Company, USA) imaging was performed at 200 kV. Western blotting was performed using antibodies against tumor susceptibility gene 101 protein (TSG101) (ab125011, Abcam, UK) and CD81 (CAC-SHI-EXO-M03, Cosmo Bio, USA), and images were acquired using an imaging instrument (Amersham Imager 600, GE Healthcare, USA).

2.3. Protein identification

The milk-derived EXO pellets were solubilized in 8 M urea (Sigma-Aldrich, USA). Protein concentration was determined using the bicinchoninic acid assay (Pierce, Thermo Fisher Scientific, USA). The protein samples were reduced with 10 mM dithiothreitol (Sigma-Aldrich, USA) at 56 °C for 30 min and alkylated with 20 mM iodoacetamide (Sigma-Aldrich, USA) at 25 °C for 30 min. To reduce the urea concentration to below 1 M, the sample was diluted tenfold and supplemented with 25 mM ammonium bicarbonate (Sigma-Aldrich, USA). The protein mixture was digested with sequencing-grade modified trypsin (Promega, USA) at 37 °C for 16 h with an enzyme:protein ratio of 1:50.

Digested peptides were analyzed utilizing a mass spectrometer (Q-Exactive Plus, Thermo Fisher Scientific, USA) coupled with a pump and autosampler system (Easy nLC-1200, Thermo Fisher Scientific, USA). The tryptic peptides were separated using a linear gradient of 5–60% acetonitrile in water containing 0.1% formic acid over 85 min. The mass spectrometer was operated in data-dependent acquisition mode with a full scan (m/z 350–2000) followed by tandem mass spectrometry (MS/MS) of the top 20 precursor ions per cycle. The acquired MS/MS spectra were searched against the UniProt *Bos taurus* (bovine) protein database (released June 2025; 59,260 sequences) using SEQUEST software in Proteome Discoverer (version 2.5, Thermo Fisher Scientific, USA). The search parameters allowed for up to two missed trypsin cleavages. Peptide mass tolerances were set to 10 ppm for precursor ions and 0.02 Da for fragment ions. Fixed modification was set as carbamidomethylation at cysteine

(+57.021 Da), and variable modification as oxidation at methionine (+15.995 Da).

2.4. MicroRNA analysis

Total miRNAs were extracted using TRIzol reagent (Invitrogen, USA) according to the manufacturer's instructions. Overall, exosomal miRNA analysis was performed by EBiogen (Seoul, Republic of Korea). The identified miRNAs were further analyzed using miRNet (https://www.mirnet.ca/).

2.5. Fabrication of exosome-coated scaffolds

Polycaprolactone was loaded into a syringe and melted in the heating jacket of a 3D printer at 100 °C. After printing, the scaffolds were uniformly cut into 6 × 6 mm squares using a surgical blade. The cut scaffolds were then immersed in dopamine hydrochloride solution and stirred for 16 h to form a PDA coating. Following coating, the PDA-modified scaffolds were rinsed with distilled water (DW) to remove residual reagents and air-dried in a laminar-flow clean bench. Each dried scaffold was then seeded with 50 μL of milk-derived EXO suspension (2 μg/mL) and incubated at 3 °C for 24 h.

2.6. Scaffold characterization

The surface morphology of each scaffold was examined using field-emission scanning electron microscopy (SEM; S-4800, Hitachi, Japan) after sputter coating with platinum. Water contact angle measurements were performed at room temperature to evaluate the surface hydrophilicity of each scaffold using a contact-angle goniometer (DSA25, Krüss, Germany). The surface chemical composition of each scaffold was analyzed using Fourier transform infrared (FTIR) spectroscopy (Tensor 27, Bruker Optics, Germany).

Compression testing was performed on individual scaffolds (6 mm × 6 mm × 2 mm) using a universal testing machine (RB301 UNITECH-M, R&B Inc., Republic of Korea) equipped with a 200 kN load cell, operated at a constant cross-head rate of 5 mm/min to evaluate mechanical properties.

2.7. Preparation of cell-seeded scaffolds

Human osteosarcoma cells (MG-63; CRL-1427, ATCC, United states) were cultured in DMEM supplemented with 10% FBS and 1% penicillin. PCL and PDA scaffolds were sterilized in 70% ethanol for 1 min, then washed several times with PBS to remove residual ethanol and reagents. Each scaffold was seeded with 5×10^5 cells. To enhance cell attachment, the cell suspension was dropped repeatedly onto the center of the scaffold. The cell-seeded scaffolds were incubated at 37 °C in an atmosphere containing 5% CO_2. To induce osteogenic differentiation, the cell-seeded scaffolds were cultured in MEM-α supplemented with 10% FBS, 1% penicillin, 0.1 μM dexamethasone, 10 μM L-ascorbic acid, and 10 mM β-glycerophosphate.

2.8. Cell viability and proliferation

Cell viability on each scaffold was assessed using a viability/cytotoxicity kit (L3224 LIVE/DEAD™, Invitrogen, USA). Cultured scaffolds were washed three times with PBS, then incubated at 37 °C for 1 h in staining solution containing calcein acetoxymethyl ester and ethidium homodimer-1. Live and dead cells were visualized using fluorescence microscopy (Eclipse Ti, Nikon, Japan).

Cell proliferation was evaluated using water-soluble tetrazolium-1 (WST-1) assay (Premix WST-1 Cell Proliferation Assay System, Takara, Japan). WST-1 solution was diluted 1:10 in DMEM, and the resulting mixture was added to the cultured scaffolds. After incubation at 37 °C for 30 min, the absorbance at 450 nm was measured using a microplate reader (Infinite® M Plex, Tecan, Switzerland).

2.9. Osteogenic differentiation and mineralization

Osteogenic differentiation was assessed by ALP assay using a commercial kit (MK301, TRACP & ALP Assay Kit, Takara, Japan) in scaffolds cultured in MEM-α. The scaffolds were first washed with PBS, and the cells were lysed using radioimmunoprecipitation assay Buffer (Pierce, Thermo Fisher Scientific, USA), then stored at −80 °C. Cell membranes were disrupted by repeated freeze–thaw cycling. The lysate was mixed with p-nitrophenyl phosphate solution at a 1:1 ratio and incubated at 37 °C for 30 min. The reaction was terminated by adding 0.9 N sodium hydroxide, and absorbance was measured at 405 nm using a microplate reader (Infinite® M Plex, Tecan, Switzerland). ALP activity was normalized relative to total DNA content using a dsDNA Assay Kit (P7859, Quant-iT™ PicoGreen™, Invitrogen, USA), allowing correlation with cell number.

The mineralization of cells in each scaffold was evaluated by staining with Alizarin Red S (ARS). Cell-seeded scaffolds were incubated in MEM-α at 37 °C for 14 days and washed several times with DW to remove residual medium. The differentiated cells in the scaffolds were fixed in 4% paraformaldehyde for 20 min at room temperature, then washed three times with DW. The cells were stained with ARS solution for 45 min in the dark. After staining, the samples were visually inspected to assess the extent of mineralization in each scaffold.

2.10. Statistical analysis

All quantitative data are presented as the mean ± standard

deviation. Statistical comparisons were performed using one-way analysis of variance (ANOVA) followed by Tukey's post hoc test. The statistical significance was set at $^{*}p < 0.05$, $^{**}p < 0.01$, and $^{***}p < 0.001$. Statistical analysis was conducted using OriginPro (2025, OriginLab Corporation, USA).

3. Results and discussion

3.1. Milk-derived exosome isolation and characterization

Milk-derived EXOs were isolated from acetic acid-treated whey using ultracentrifugation. Nanoparticle analysis revealed a distinct peak in particle concentration, with most particles being 50–150 nm in diameter. The highest concentration was observed at approximately 100 nm, within the typical size range for EXOs.[24] These observations indicated that the isolation protocol effectively enriched a population of nanosized vesicles, which was further confirmed using size-exclusion chromatography–high-performance liquid chromatography analysis (Figure S1). Quantitative analysis showed a mode concentration of 8.58 $\times 10^{11}$ particles/mL at 100 nm (Figure 2A).

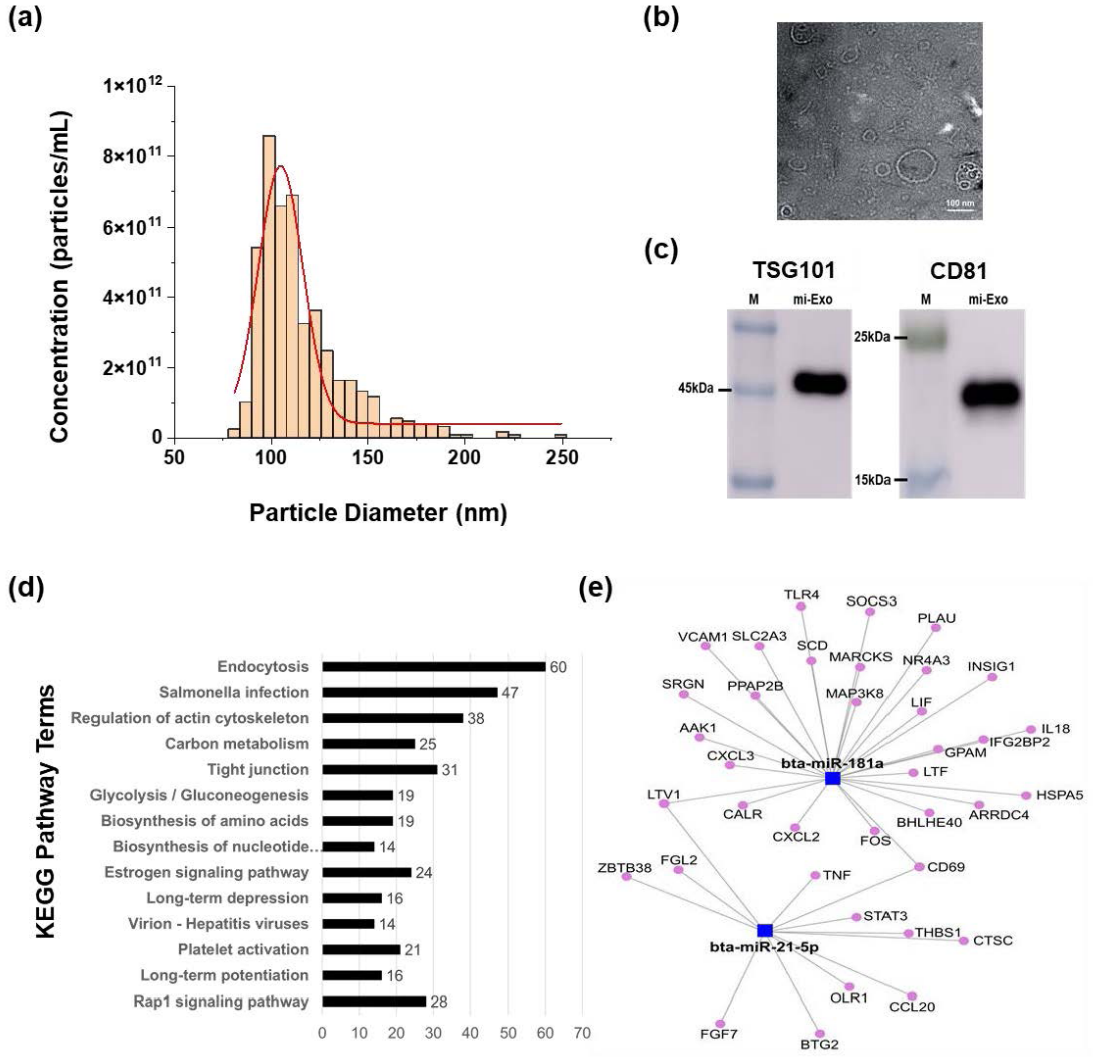

Figure 2. Characterization, proteomic, and transcriptomic analysis of milk-derived exosomes (EXOs). (A) Size distribution and concentration of EXOs. (B) Morphological data obtained by cryo-electron microscopy (scale bar: 100 nm; magnification: 100 nm). (C) Western blotting of exosomal marker proteins: milk-derived EXO cytosolic protein (tumor susceptibility gene 101 protein, TSG101) and transmembrane protein (CD81). (D) Bar plot of significant Kyoto Encyclopedia of Genes and Genomes (KEGG) pathway terms. (E) MicroRNA (miRNA) network using 31 highly expressed milk-derived EXO miRNAs. The miRNAs involved in the network are shown in blue. Related genes are shown in pink.

In cryo-EM, the vesicles appeared as spherical particles with a clear lipid bilayer, consistent with the morphological characteristics of EXOs. The scale of these vesicles matched the NTA measurements, reinforcing the conclusion that the isolated particles fell within the expected size range of EXOs (Figure 2B). Western blotting analysis provided definitive molecular evidence for the identity of the isolated milk-derived EXOs, with clear bands for the TSG101 and CD81 (Figure 2C).[23,25,26]

Taken together, the results above confirmed the purification of extracellular vesicles consistent with the size, morphology, and canonical surface markers of EXOs. This foundational step established a reliable protocol for obtaining pure milk-derived EXO preparations for subsequent proteomic and transcriptomic analyses.

3.2. Gene ontology and miRNA transcriptomic analysis of milk-derived exosomes

Gene ontology analysis was performed to characterize the protein cargo encapsulated within the isolated milk-derived EXOs (Figure S2). While the genomic data provided insights into general exosomal functions, parallel transcriptomic analysis of EXO miRNA cargo revealed a specific connection to bone metabolism. The top 31 most highly expressed miRNAs (cutoff of $p < 0.05$) were selected for further analysis, and miRNet network analysis identified bta-miR-21-5p and bta-miR-181a as key components connected to major networks (Figures 2E and S3). The normalized expression levels of the two miRNAs were 14.34 for bta-miR-21a-5p ($n = 3$) and 11.83 for bta-miR-181a ($n = 3$), corresponding to the 12th and 25th highest expression levels, respectively, among the 31 major miRNAs. Kyoto Encyclopedia of Genes and Genomes (KEGG) pathway analysis of the identified miRNAs revealed significant enrichment in the osteoclast differentiation pathway ($p_{adj} = 0.0322$; Table S1). This pathway, which is essential for bone resorption, has been associated with the regulation of several key genes, including *SOCS3*, *FOS*, and *TNF*.[27-29]

These findings suggest that milk-derived EXOs may modulate the bone remodeling microenvironment via their miRNA cargo, particularly by regulating osteoclast activity. This function is likely to play a critical role in promoting balanced bone regeneration through coordinated control of both osteoblast and osteoclast dynamics.

The results of genomic analysis of the EXO cargo revealed a diverse profile of proteins primarily involved in fundamental cellular processes, including vesicle-mediated transport, protein trafficking, and metabolic regulation. Notably, no significant enrichment was observed in pathways directly related to osteogenesis or bone formation. In contrast, transcriptomic analysis of the EXO miRNA cargo identified a critical and specific link to bone metabolism that was not evident from the genomic data. KEGG pathway enrichment analysis identified a significant overrepresentation of the osteoclast differentiation pathway.

This finding is particularly important, as it suggests a mechanism of action distinct from classical osteoinduction. Bone regeneration is dependent on the finely regulated balance between osteoblast-mediated bone formation and osteoclast-mediated bone resorption.[30,31] The presence of miRNAs targeting genes involved in osteoclast differentiation, such as *SOCS3*, *FOS*, and *TNF*, implied that milk-derived EXOs may modulate bone remodeling by regulating osteoclast activity rather than by directly stimulating osteoblasts (Table S1 and Figure S3). This points to a regulatory or immunomodulatory role for EXOs, potentially influencing the inflammatory and remodeling phases of bone healing.[32]

These findings contribute to the growing body of evidence that EXO-based therapies exert complex and context-dependent biological effects, determined by their cargo of proteins, miRNAs, and other biomolecules.[24,33] The apparent discrepancy between genomic and transcriptomic data highlights the value of a multiomics approach for comprehensive characterization of EXO function.[23,34] The results imply that milk-derived EXOs may not directly stimulate bone-forming cells but instead modulate bone resorption, a novel and potentially powerful therapeutic strategy for conditions such as non-union fractures, where dysregulation of the bone remodeling cycle is a major hindrance to healing (Figure S3).

3.3. Scaffold characterization

3.3.1. Morphology

The morphologies of 3D-printed PCL scaffolds, PDA-coated PCL scaffolds, and PDA–EXO scaffolds are shown in Figure 3A. All scaffolds were designed to have a porous architecture with a grid interval of 400 μm to enhance cell infiltration and proliferation.[35] The surface morphology of each scaffold was assessed using SEM at magnifications of 150 × and 30,000 × (Figure 3B). SEM images confirmed the uniform distribution of PDA particles on the PCL scaffold surface. High-magnification images revealed that the milk-derived EXOs used for coating had the typical spherical vesicle morphology and were heterogeneous in size.[23]

The high density of EXOs on the PDA–EXO scaffold surface was attributed to the catechol and amine functional groups of PDA that formed strong covalent and non-covalent bonds with the EXO surface and thus provided strong adhesion.[20] These adhesive properties of PDA

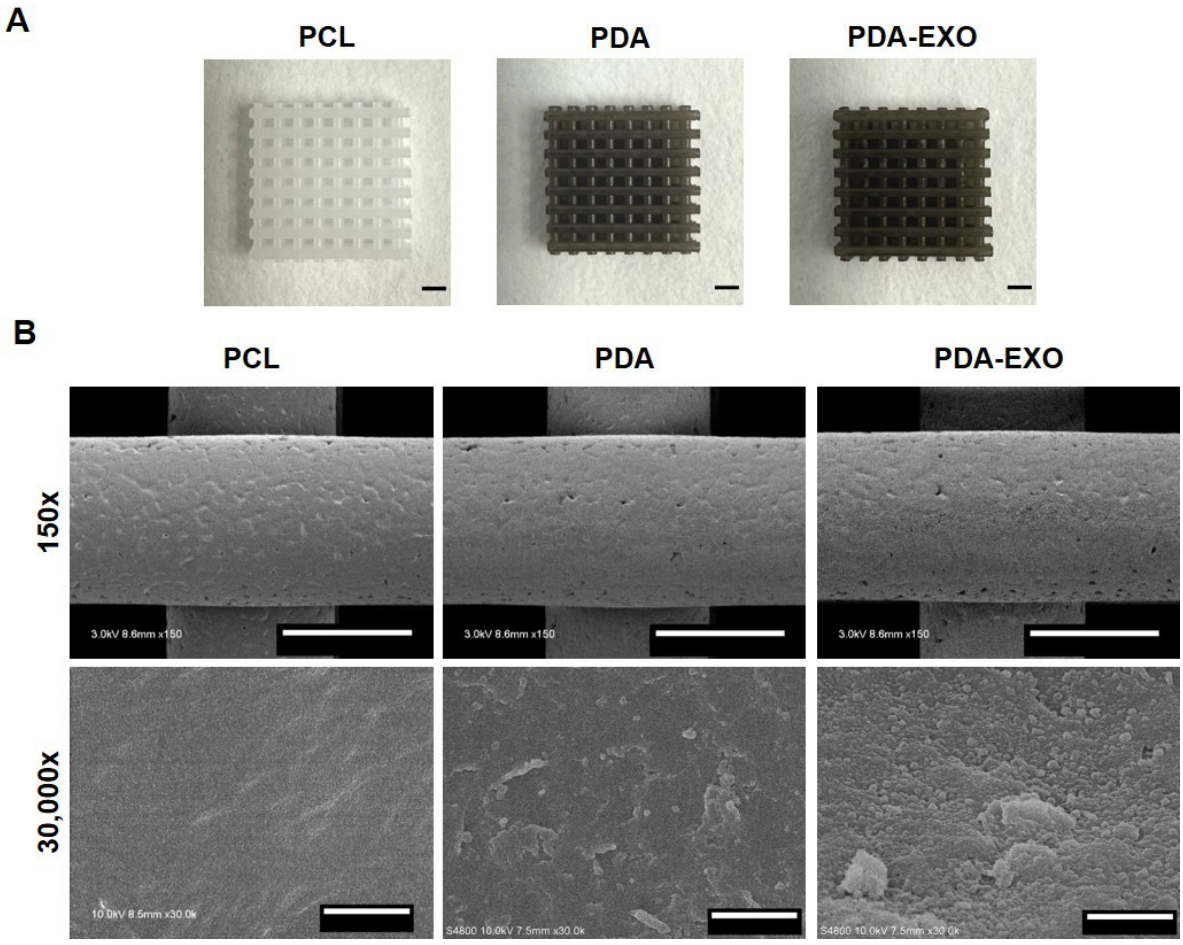

Figure 3. Fabrication and surface results of PCL, PDA, and PDA–EXO scaffolds. (A) 3D-printed and coated scaffolds (scale bar: 1 mm). (B) Scanning electron microscopy images of the surfaces of PCL, PDA, and PDA–EXO scaffolds (Scale bars: 300 μm, 1 μm; magnification: 150 ×, 30,000 ×).
Abbreviations: PCL: Polycaprolactone; PDA: Polydopamine-coated polycaprolactone; PDA–EXO: exosome-coated polydopamine-coated polycaprolactone.

promoted uniform and stable EXO immobilization with high surface density.[36] Overall, SEM analysis demonstrated the even distribution of PDA and milk EXOs on the PDA and PDA–EXO scaffolds, respectively.

3.3.2. Fourier transform infrared spectroscopy and hydrophilicity

The FTIR spectra of PCL, PDA, and PDA–EXO scaffolds are shown in Figure 4A. The PCL spectrum showed the characteristic C–H asymmetric and symmetric stretching bands at 2,979 cm^{-1} and 2,898 cm^{-1}, respectively. The peak at 1,722 cm^{-1} was attributed to C=O stretching of the ester group in PCL.[37,38] The FTIR spectrum of the PDA scaffold showed a wide peak between 3,700 cm^{-1} and 3,033 cm^{-1}, attributed to the stretching vibration of O–H groups. In addition, N–H vibration of the amine groups in PDA was observed at 1,648 cm^{-1}.[39]

The FTIR spectrum of PDA–EXO scaffold also showed the characteristic PDA peaks with an additional peak at 1,650 cm^{-1}, corresponding to the amide I band, indicating C=O stretching vibration in proteins, supporting the presence of milk-derived EXOs.[40]

A hydrophilic scaffold surface can enhance cell adhesion by promoting protein adsorption and cell attachment.[17] The PCL scaffold had a water contact angle of 74.2°, confirming its hydrophobic surface, while the PDA-coated scaffold absorbed water and had a contact angle of 0° (Figure 4B).[41] These results indicate that the surface of the PDA-coated scaffolds became hydrophilic, which was expected to enhance cell adhesion.[17,42]

2.4. Mechanical properties

The compressive properties of PCL, PDA, and PDA–EXO

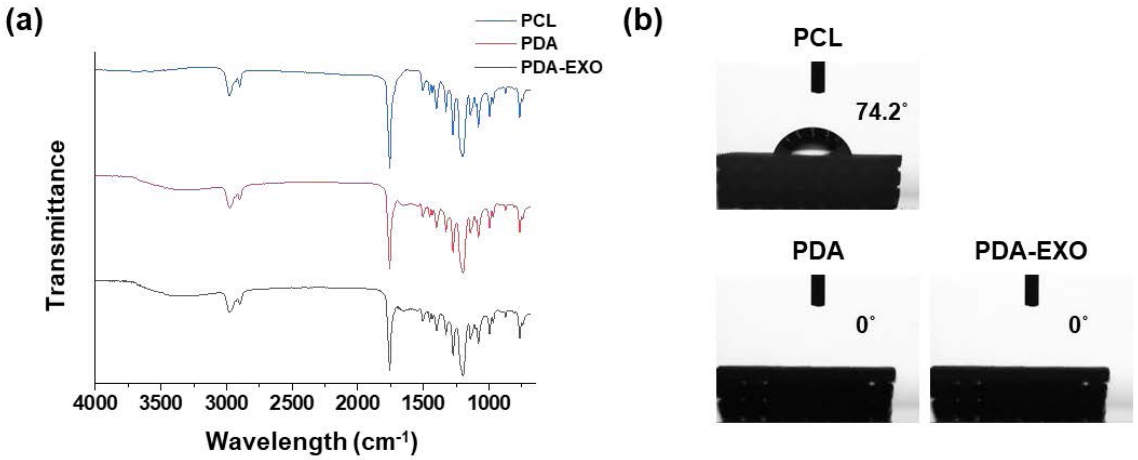

Figure 4. Surface characterization of PCL, PDA, and PDA–EXO scaffolds. (A) Fourier transform infrared spectra of PCL, PDA, and PDA–EXO scaffolds. (B) Contact angle images of each scaffold.
Abbreviations: PCL: Polycaprolactone; PDA: Polydopamine-coated polycaprolactone; PDA–EXO: exosome-coated polydopamine-coated polycaprolactone.

scaffolds are shown in Figure 5. As shown in Figure 5A, there were no significant differences in the stress–strain curves among the groups. In addition, there were also no marked differences in Young's modulus among PCL, PDA, and PDA–EXO scaffolds (Figure 5B). These results indicate that PDA coating and EXO immobilization had no significant effect on the mechanical properties of the PCL scaffolds. While PDA coating improved the hydrophilicity of the scaffold surface layer and milk-derived EXOs improved the bioactivity of the scaffold surface, both functioned as surface modifications without compromising the mechanical properties of the PCL scaffolds.[43,44]

3.5. Cell viability and proliferation

To assess cell viability and attachment on the scaffolds, live/dead cell staining was performed after incubation. As shown in Figure 6A, all scaffold groups exhibited a higher proportion of live than dead cells, attributed to the inherent biocompatibility and nontoxicity of the PCL scaffold.[45] On days 4 and 7, PDA-coated scaffolds had higher cell viability than PCL scaffolds, while the PDA–EXO group exhibited the highest viability at both time points. These results

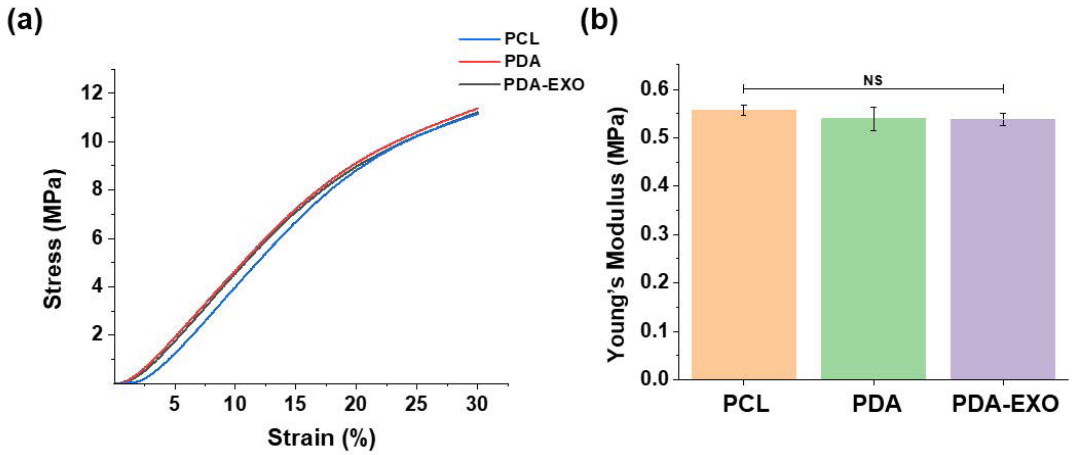

Figure 5. Mechanical properties of PCL, PDA, and PDA–EXO scaffolds. (A) Compression stress–strain curves of PCL, PDA, and PDA–EXO scaffolds. (B) Young's modulus of each scaffold. Note: $n = 3$.
Abbreviations: NS: No significant difference; PCL: Polycaprolactone; PDA: Polydopamine-coated polycaprolactone; PDA–EXO: exosome-coated polydopamine-coated polycaprolactone.

indicate that the hydrophobic PCL surface was successfully modified to a hydrophilic one by PDA coating, enhancing protein adsorption and cell adhesion.[36,43,46] As previous studies showed that milk-derived EXOs can enhance cell adhesion and proliferation by activating proliferation-associated signaling pathways, the superior performance of the PDA–EXO scaffolds was attributed to the synergistic effects of PDA-induced hydrophilicity and EXO-mediated bioactivity, resulting in improved biocompatibility and cell viability.[44,47]

Cell proliferation was further evaluated using WST-1 assays on days 4 and 7 (Figure 6B). Cell proliferation was higher on PDA-coated scaffolds than on unmodified PCL scaffolds, attributed to the improved surface properties. PDA–EXO scaffolds showed the greatest cell proliferation among the groups examined. These results confirm that the PDA–EXO scaffolds provided highly biocompatible conditions that supported cell growth.

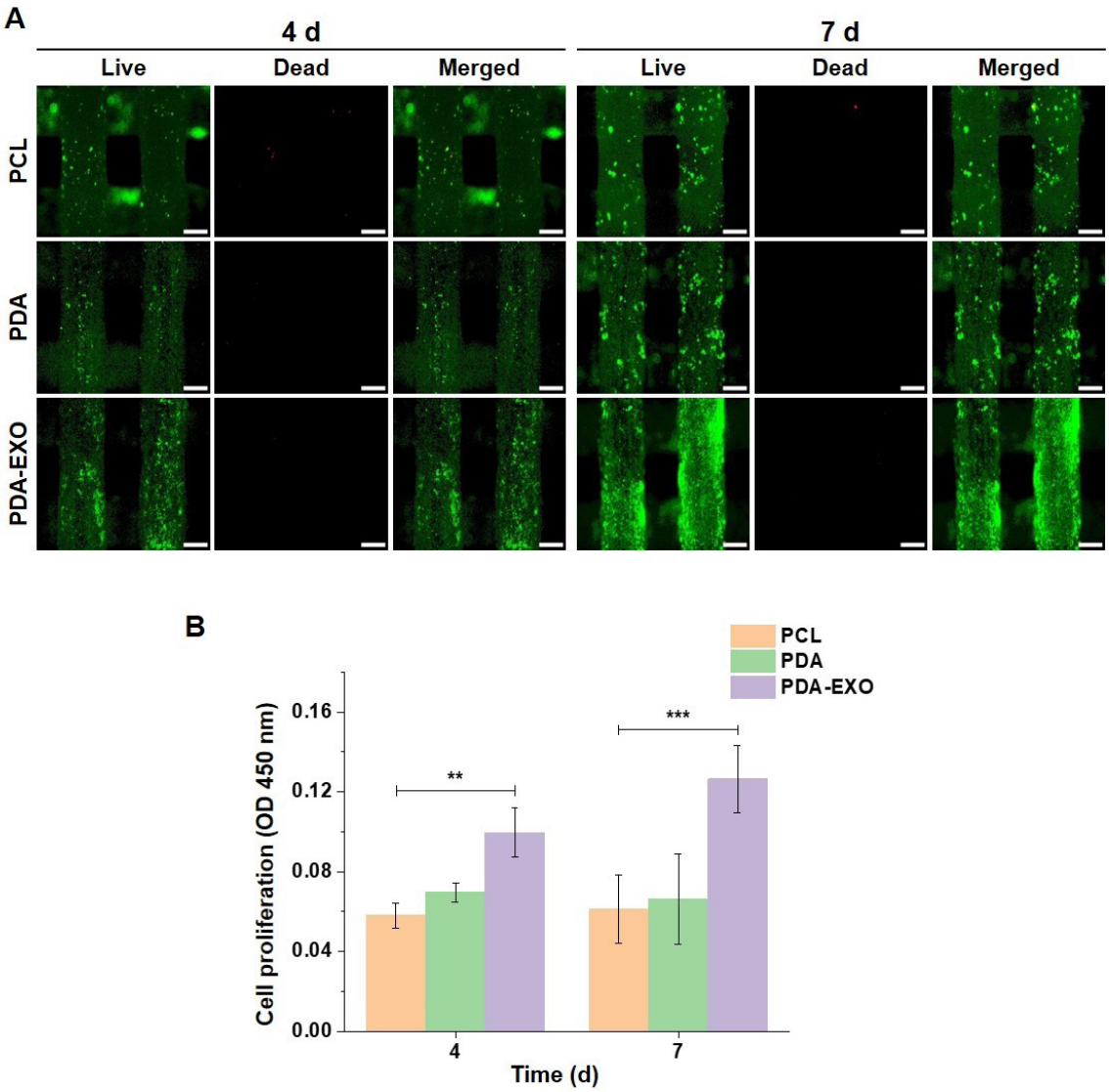

Figure 6. Cell viability and proliferation of cultured cells in PCL, PDA, and PDA–EXO scaffolds. (A) Live/dead assay of cells cultured for 4 and 7 days (scale bar: 200 μm, magnification: 4×). (B) Water-soluble tetrazolium-1 assay of cells cultured for 4 and 7 days. Notes: $n = 4$; $^{**}p < 0.01$; $^{***}p < 0.001$.
Abbreviations: OD: Optical density; PCL: Polycaprolactone; PDA: Polydopamine-coated polycaprolactone; PDA–EXO: exosome-coated polydopamine-coated polycaprolactone.

3.6. Osteogenic differentiation and mineralization

Alkaline phosphatase activity is a commonly used early marker of osteogenic differentiation, as increased ALP activity reflects the early stage of mineralization by producing inorganic phosphate for hydroxyapatite formation.[48,49] As shown in Figure 7A, ALP activity increased over time in all cultured scaffold groups. PDA-coated scaffolds had higher ALP activity than PCL, and PDA–EXO scaffolds consistently showed the highest ALP activity at both time points examined. These findings suggest that the PDA coating enhanced osteogenic differentiation by improving the scaffold's surface biocompatibility.[18,19,36] Moreover, the increased ALP activity observed in the PDA–EXO group was attributed to the presence of osteogenesis-related miRNAs and proteins within milk-derived EXOs, which enhanced osteogenic differentiation.[43,50] Thus, EXO functionalization of the scaffolds not only significantly increases early osteogenic signaling but may also contribute to matrix mineralization.

To assess mineralization, ARS staining was performed on day 14 to detect calcium deposition in the scaffolds. Mineralization is the deposition of calcium and phosphate in the extracellular matrix, resulting in the formation of hydroxyapatite. Thus, calcium deposition detected by ARS staining was used to assess active mineralization and to indicate that osteoblasts within the scaffolds had progressed toward matrix maturation.[51] As shown in Figure 7B, calcium deposition was highest in the PDA–EXO group, which is consistent with the results of the ALP assays.

Taken together with previous results showing enhanced cell viability and proliferation, these findings support the conclusion that milk-derived EXOs contribute significantly to bone formation and regeneration by

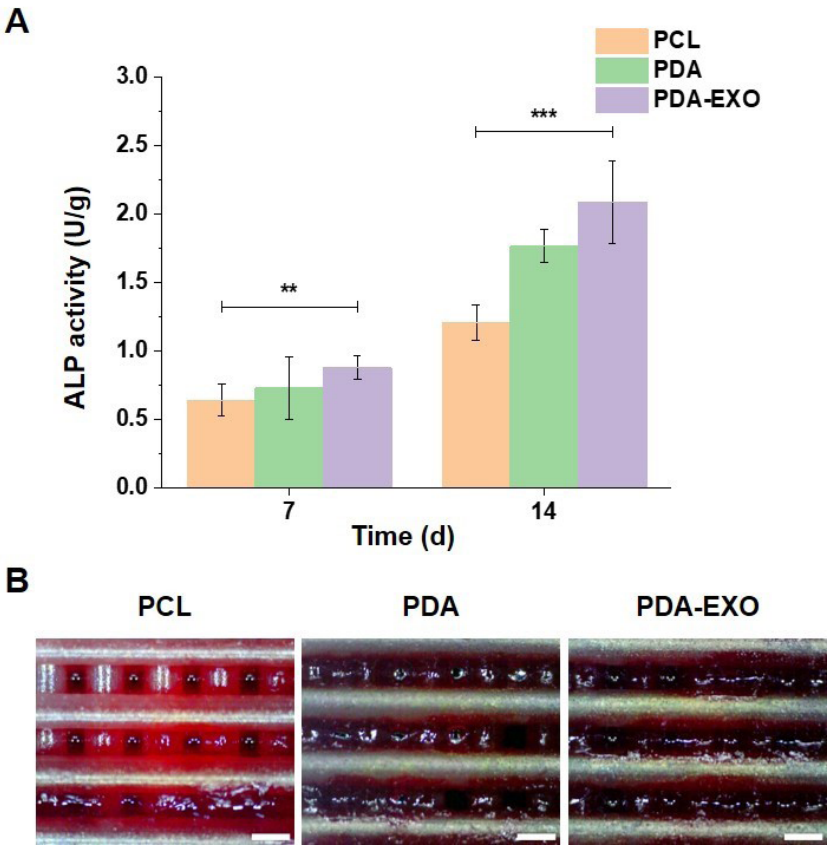

Figure 7. Osteogenic differentiation and mineralization of cultured cells in PCL, PDA, and PDA–EXO scaffolds. (A) ALP activity of cells cultured for 7 and 14 days. (B) Alizarin red staining of the cultured scaffolds on day 14 (scale bar: 400 μm; magnification: 400 μm). Notes: $n = 5$; $^{**}p < 0.01$; $^{***}p < 0.001$. Abbreviations: ALP: Alkaline phosphatase; PCL: Polycaprolactone; PDA: Polydopamine-coated polycaprolactone; PDA–EXO: exosome-coated polydopamine-coated polycaprolactone.

promoting both early osteogenic differentiation and late-stage mineralization.

4. Conclusion

A functional scaffold for bone regeneration was developed by immobilizing milk-derived EXOs rich in miRNAs associated with bone regeneration onto PDA-coated PCL scaffolds fabricated using 3D printing to achieve an interconnected porous structure. These PDA–EXO scaffolds were shown to have a uniform distribution of EXOs.

Compared to unmodified PCL scaffolds, PDA–EXO scaffolds retained their mechanical integrity while significantly enhancing cell proliferation due to the improved surface hydrophilicity by the PDA coating and bioactive stimulation from the EXOs. PDA–EXO scaffolds demonstrated the highest levels of osteogenic differentiation and mineralization among those examined, attributed to the synergistic effects of PDA and EXO osteoinductive properties. These findings imply that PDA–EXO scaffolds can provide a favorable microenvironment for cell growth and bone tissue formation. Therefore, the immobilization of milk-derived EXOs onto PDA-coated scaffolds represents a promising, cell-free therapeutic strategy for bone tissue engineering.

Acknowledgments

None

Funding

This study was supported by the National Research Foundation (NRF; No. NRF-RS-2024-00411892) and the National Research Council of Science & Technology (CRC22021- 200) funded by the Korean government. It was also supported by the Materials and Components Technology Development Program (RS-2024-00403563 and RS-2024-00431712) of the Korea Evaluation Institute of Industrial Technology (KEIT) grant funded by the Korea government (MOTIR).

Conflict of interest

The authors declare they have no competing interests.

Author contributions

Conceptualization: Ji-Young Ahn, Su A Park
Formal analysis: Jae Jong Lee
Investigation: Gna Ahn, Hye-Jung Kim
Methodology: Junhyoung Ahn, Hyungjun Lim
Writing–original draft: Ilwoo Jun
Writing–review & editing: Su A Park

Ethics approval and consent to participate

Not applicable.

Consent for publication

Not applicable.

Availability of data

All data used in the analyses are provided in the main text and the supplementary materials.

References

1. Roszkowski S. Therapeutic potential of mesenchymal stem cell-derived exosomes for regenerative medicine applications. *Clin Exp Med*. 2024;24(1):46.

   doi: 10.1007/s10238-023-01282-z

2. Oliveira MC, Arntz OJ, Blaney Davidson EN, *et al*. Milk extracellular vesicles accelerate osteoblastogenesis but impair bone matrix formation. *J Nutr Biochem*. 2016;30:74-84.

   doi: 10.1016/j.jnutbio.2015.11.017

3. Jang H, Kim H, Kim EH, *et al*. Post-insertion technique to introduce targeting moieties in milk exosomes for targeted drug delivery. *Biomater Res*. 2023;27(1):124.

   doi: 10.1186/s40824-023-00456-w

4. Go G, Jeon J, Lee G, Lee JH, Lee SH. Bovine milk extracellular vesicles induce the proliferation and differentiation of osteoblasts and promote osteogenesis in rats. *J Food Biochem*. 2021;45(4):e13705.

   doi: 10.1111/jfbc.13705

5. Zhao P, Xiao L, Peng J, Qian YQ, Huang CC. Exosomes derived from bone marrow mesenchymal stem cells improve osteoporosis through promoting osteoblast proliferation via MAPK pathway. *Eur Rev Med Pharmacol Sci*. 2018;22(12):3962-3970.

   doi: 10.26355/eurrev_201806_15280

6. Preethi Soundarya S, Haritha Menon A, Viji Chandran S, Selvamurugan N. Bone tissue engineering: Scaffold preparation using chitosan and other biomaterials with different design and fabrication techniques. *Int J Biol Macromol*. 2018;119:1228-1239.

   doi: 10.1016/j.ijbiomac.2018.08.056

7. Chia HN, Wu BM. Recent advances in 3D printing of biomaterials. *J Biol Eng*. 2015;9(1):4.

   doi: 10.1186/s13036-015-0001-4

8. Karanth D, Song K, Martin ML, *et al*. Towards resorbable 3D-printed scaffolds for craniofacial bone regeneration. *Orthod Craniofac Res*. 2023;26(suppl 1):188-195.

doi: 10.1111/ocr.12645

9. Lee SS, Du X, Kim I, Ferguson SJ. Scaffolds for bone-tissue engineering. *Matter*. 2022;5(9):2722-2759.

   doi: 10.1016/j.matt.2022.06.003

10. Li L, Li J, Guo J, *et al*. 3D molecularly functionalized cell-free biomimetic scaffolds for osteochondral regeneration. *Adv Funct Mater*. 2019;29(6):1807356.

    doi: 10.1002/adfm.201807356

11. Deng L, Liu Y, Wu Q, *et al*. Exosomes to exosome-functionalized scaffolds: a novel approach to stimulate bone regeneration. *Stem Cell Res Ther*. 2024;15(1):407.

    doi: 10.1186/s13287-024-04024-4

12. Xu H, Chai Q, Xu X, *et al*. Exosome-functionalized Ti6Al4V scaffolds promoting osseointegration by modulating endogenous osteogenesis and osteoimmunity. *ACS Appl Mater Interfaces*. 2022;14(41):46161-46175.

    doi: 10.1021/acsami.2c11102

13. Shenoda BB, Ajit SK. Modulation of immune responses by exosomes derived from antigen-presenting cells. *Clin Med Insights Pathol*. 2016;9(suppl 1):1-8.

    doi: 10.4137/CPath.S39925

14. Hajiali F, Tajbakhsh S, Shojaei A. Fabrication and properties of polycaprolactone composites containing calcium phosphate-based ceramics and bioactive glasses in bone tissue engineering: A Review. *Polym Rev*. 2018;58(1):164-207.

    doi: 10.1080/15583724.2017.1332640

15. Ebrahimi Z, Irani S, Ardeshirylajimi A, Seyedjafari E. Enhanced osteogenic differentiation of stem cells by 3D printed PCL scaffolds coated with collagen and hydroxyapatite. *Sci Rep*. 2022;12(1):12359.

    doi: 10.1038/s41598-022-15602-y

16. Tolabi H, Bakhtiary N, Sayadi S, *et al*. A critical review on polydopamine surface-modified scaffolds in musculoskeletal regeneration. *Front Bioeng Biotechnol*. 2022;10:1008360.

    doi: 10.3389/fbioe.2022.1008360

17. Tsai WB, Chen WT, Chien HW, Kuo WH, Wang MJ. Poly(dopamine) coating of scaffolds for articular cartilage tissue engineering. *Acta Biomater*. 2011;7(12):4187-4194.

    doi: 10.1016/j.actbio.2011.07.024

18. Lee DJ, Tseng HC, Wong SW, Wang Z, Deng M, Ko CC. Dopaminergic effects on in vitro osteogenesis. *Bone Res*. 2015;3(1):15020.

    doi: 10.1038/boneres.2015.20

19. Wang J, Cui Y, Zhang B, *et al*. Polydopamine-modified functional materials promote bone regeneration. *Mater Des*. 2024;238:112655.

    doi: 10.1016/j.matdes.2024.112655

20. Zhang P, He M, Zeng Y. Ultrasensitive microfluidic analysis of circulating exosomes using a nanostructured graphene oxide/polydopamine coating. *Lab Chip*. 2016;16(16):3033-3042.

    doi: 10.1039/C6LC00279J

21. Li W, Liu Y, Zhang P, *et al*. Tissue-engineered bone immobilized with human adipose stem cells-derived exosomes promotes bone regeneration. *ACS Appl Mater Interfaces*. 2018;10(6):5240-5254.

    doi: 10.1021/acsami.7b17620

22. Gao Y, Yuan Z, Yuan X, *et al*. Bioinspired porous microspheres for sustained hypoxic exosomes release and vascularized bone regeneration. *Bioact Mater*. 2022;14:377-388.

    doi: 10.1016/j.bioactmat.2022.01.041

23. Ahn G, Kim YH, Ahn JY. Multifaceted effects of milk-exosomes (Mi-Exo) as a modulator of scar-free wound healing. *Nanoscale Adv*. 2021;3(2):528-537.

    doi: 10.1039/D0NA00665C

24. Kalluri R, LeBleu VS. The biology, function, and biomedical applications of exosomes. *Science*. 2020;367(6478):eaau6977.

    doi: 10.1126/science.aau6977

25. Kalra H, Adda CG, Liem M, *et al*. Comparative proteomics evaluation of plasma exosome isolation techniques and assessment of the stability of exosomes in normal human blood plasma. *Proteomics*. 2013;13(22):3354-3364.

    doi: 10.1002/pmic.201300282

26. Deng F, Miller J. A review on protein markers of exosome from different bio-resources and the antibodies used for characterization. *J Histotechnol*. 2019;42(4):226-239.

    doi: 10.1080/01478885.2019.1646984

27. Sims NA. The JAK1/STAT3/SOCS3 axis in bone development, physiology, and pathology. *Exp Mol Med*. 2020;52(8):1185-1197.

    doi: 10.1038/s12276-020-0445-6

28. Asagiri M, Takayanagi H. The molecular understanding of osteoclast differentiation. *Bone*. 2007;40(2):251-264.

    doi: 10.1016/j.bone.2006.09.023

29. Kitaura H, Kimura K, Ishida M, Kohara H, Yoshimatsu M, Takano-Yamamoto T. Immunological reaction in TNF-α-mediated osteoclast formation and bone resorption in vitro and in vivo. *Clin Dev Immunol*. 2013;2013:181849.

    doi: 10.1155/2013/181849

30. Wang L, You X, Zhang L, Zhang C, Zou W. Mechanical regulation of bone remodeling. *Bone Res*. 2022;10(1):16.

    doi: 10.1038/s41413-022-00190-4

31. Mulari MTK, Qu Q, Härkönen PL, Väänänen HK. Osteoblast-like cells complete osteoclastic bone resorption and form new mineralized bone matrix in vitro. *Calcif Tissue Int*. 2004;75(3):253-261.

    doi: 10.1007/s00223-004-0172-3

32. Zhou Q, Li M, Wang X, *et al*. Immune-related microRNAs are abundant in breast milk exosomes. *Int J Biol Sci*. 2012;8(1):118-123.

    doi: 10.7150/ijbs.8.118

33. Huda MN, Nafiujjaman M, Deaguero IG, *et al*. Potential use of exosomes as diagnostic biomarkers and in targeted drug delivery: progress in clinical and preclinical applications. *ACS Biomater Sci Eng*. 2021;7(6):2106-2149.

    doi: 10.1021/acsbiomaterials.1c00217

34. Busso-Lopes AF, Carnielli CM, Winck FV, *et al*. A reductionist approach using primary and metastatic cell-derived extracellular vesicles reveals hub proteins associated with oral cancer prognosis. *Mol Cell Proteomics*. 2021;20:100118.

    doi: 10.1016/j.mcpro.2021.100118

35. Deliormanlı AM, Atmaca H. Effect of pore architecture on the mesenchymal stem cell responses to graphene/polycaprolactone scaffolds prepared by solvent casting and robocasting. *J Porous Mater*. 2020;27(1):49-61.

    doi: 10.1007/s10934-019-00791-1

36. Lee H, Han G, Na Y, *et al*. 3D-Printed Tissue-Specific Nanospike-Based Adhesive Materials for Time-Regulated Synergistic Tumor Therapy and Tissue Regeneration In Vivo. *Adv Funct Mater*. 2024;34(48):2406237.

    doi: 10.1002/adfm.202406237

37. Bružauskaitė I, Bironaitė D, Bagdonas E, Bernotienė E. Scaffolds and cells for tissue regeneration: different scaffold pore sizes—different cell effects. *Cytotechnology*. 2016;68(3):355-369.

    doi: 10.1007/s10616-015-9895-4

38. Peng L, Pan Y, Liu Q, *et al*. Hierarchically functionalized PCL/CS with synergistic PDA-mediated antioxidant therapy and NGF-activated neurogenesis for spinal cord injury regeneration. *J Biomater Sci Polym Ed*. Published online August 3, 2025.

    doi: 10.1080/09205063.2025.2542479

39. Shariati A, Ebrahimi T, Babadinia P, Shariati FS, Ahangari Cohan R. Synthesis and characterization of Gd3+-loaded hyaluronic acid-polydopamine nanoparticles as a dual contrast agent for CT and MRI scans. *Sci Rep*. 2023;13(1):4520.

    doi: 10.1038/s41598-023-31252-0

40. Baddela VS, Nayan V, Rani P, Onteru SK, Singh D. Physicochemical biomolecular insights into buffalo milk-derived nanovesicles. *Appl Biochem Biotechnol*. 2016;178(3):544-557.

    doi: 10.1007/s12010-015-1893-7

41. Cho SJ, Jung SM, Kang M, Shin HS, Youk JH. Preparation of hydrophilic PCL nanofiber scaffolds via electrospinning of PCL/PVP-b-PCL block copolymers for enhanced cell biocompatibility. *Polymer*. 2015;69:95-102.

    doi: 10.1016/j.polymer.2015.05.037

42. Rim NG, Kim SJ, Shin YM, *et al*. Mussel-inspired surface modification of poly(l-lactide) electrospun fibers for modulation of osteogenic differentiation of human mesenchymal stem cells. *Colloids Surf B Biointerfaces*. 2012;91:189-197.

    doi: 10.1016/j.colsurfb.2011.10.057

43. Wu Y, Zhang Y, Zhang R, Chen S. Preparation and properties of antibacterial polydopamine and nano-hydroxyapatite modified polyethylene terephthalate artificial ligament. *Front Bioeng Biotechnol*. 2021;9:630745.

    doi: 10.3389/fbioe.2021.630745

44. Kyung Kim D, Lee S, Kim M, Jeong Y, Lee S. Exosome-coated silk fibroin 3D-scaffold for inducing osteogenic differentiation of bone marrow derived mesenchymal stem cells. *Chem Eng J*. 2021;406:127080.

    doi: 10.1016/j.cej.2020.127080

45. Serrano MC, Pagani R, Vallet-Regí M, *et al*. In vitro biocompatibility assessment of poly(ε-caprolactone) films using L929 mouse fibroblasts. *Biomaterials*. 2004;25(25):5603-5611.

    doi: 10.1016/j.biomaterials.2004.01.037

46. Cai S, Wu C, Yang W, Liang W, Yu H, Liu L. Recent advance in surface modification for regulating cell adhesion and behaviors. *Nanotechnol Rev*. 2020;9(1):971-989.

    doi: 10.1515/ntrev-2020-0076

47. Liang W, Han B, Hai Y, Sun D, Yin P. Mechanism of action of mesenchymal stem cell-derived exosomes in the intervertebral disc degeneration treatment and bone repair and regeneration. *Front Cell Dev Biol*. 2022;9:833840.

    doi: 10.3389/fcell.2021.833840

48. Cannalire G, Pilloni S, Esposito S, Biasucci G, Di Franco A, Street ME. Alkaline phosphatase in clinical practice in childhood: Focus on rickets. *Front Endocrinol*. 2023;14:1111445.

    doi: 10.3389/fendo.2023.1111445

49. Meesuk L, Suwanprateeb J, Thammarakcharoen F, *et al*. Osteogenic differentiation and proliferation potentials of human bone marrow and umbilical cord-derived mesenchymal stem cells on the 3D-printed hydroxyapatite scaffolds. *Sci Rep*. 2022;12(1):19509.

doi: 10.1038/s41598-022-24160-2

50. Zhang M, Li Y, Feng T, *et al*. Bone Engineering Scaffolds with Exosomes: A Promising Strategy for Bone Defects Repair. *Front Bioeng Biotechnol*. 2022;10:920378.

doi: 10.3389/fbioe.2022.920378

51. Hany E, Yahia S, Elsherbeny MF, *et al*. Evaluation of the osteogenic potential of rat adipose-derived stem cells with different polycaprolactone/alginate-based nanofibrous scaffolds: an in vitro study. *Stem Cell Investig*. 2020;7:14.

doi: 10.21037/sci-2020-019